Chemical Infiltration during Atomic Layer Deposition: Metalation of Porphyrins as Model Substrates**

Lianbing Zhang,* Avinash J. Patil, Le Li, Angelika Schierhorn, Stephen Mann, Ulrich Gösele, and Mato Knez*

Atomic layer deposition (ALD) is a gas-phase deposition process based on successive self-terminating gas–solid reactions. During the process, the template substrate is exposed to precursor molecules from the gas phase, which ideally promotes adsorption of a monolayer on the surface. After purging the excess precursor and subsequent exposure to a second gaseous precursor, reaction on the surface of the substrate leads to formation of a layer of the desired material. The layer thickness is controlled by the number of the reaction cycles. Owing to the precise thickness control and broad range of operating temperatures, ALD has recently been used for coating various structures, including thermally and chemically sensitive organic and biological macromolecules.[1–3] Much work has also been performed to develop new precursors and new processes to increase the versatility of ALD. For example, a number of studies have been devoted to the investigation of the interface chemistry during the deposition process to achieve better control over the deposition rate and the area selectivity of the deposition. Several reviews about ALD have been recently published.[4–6]

To date, only little attention has been paid to the chemical interactions between the precursors and the substrate underneath the macroscopic interface formed during the ALD process. It is essential to understand such interactions, particularly as an increasing number of organic soft materials are being used in ALD processes to fulfill various tasks: for example, as masks for area-selective deposition,[1] scaffolds for hybrid material fabrication,[7] or templates for the fabrication of nanostructures.[8] Such materials normally contain various functional groups that are potentially reactive with ALD precursors. Precursors can diffuse through polymer layers during the ALD process, but the chemical interactions between the precursors and the substrate during the diffusion process has only been proposed.[3, 9]

Herein, we use J-aggregate nanostructures composed of *meso*-tetra(*p*-phenylsulfonato)porphyrin (TSPP) or *meso*-tetraphenylporphyrin (H₂TPP) as model substrates for standard metal oxide ALD, and show for the first time that the

TSPP   H₂TPP
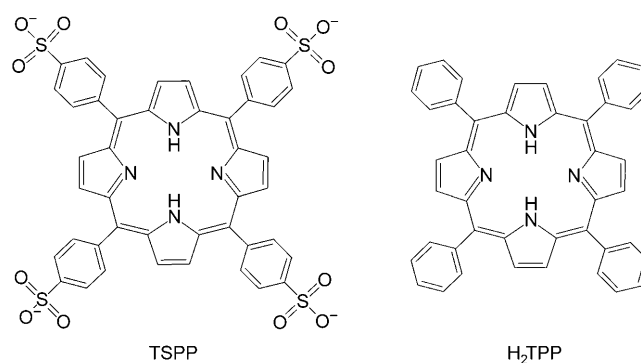
precursor can infiltrate the substrate at the molecular level and induce site-specific metalation. Self-assembly of protonated TSPP molecules into J-aggregate nanotapes occurs through electrostatic interactions between the negatively charged sulfonato groups and positively charged pyrrole amine groups,[10] which are also potential active sites for interactions with ALD precursors. Moreover, the protonated and deprotonated monomer and the J-aggregate of TSPP have distinct light absorption profiles,[11] which provides a convenient method for analysis. Specifically, we show that processing the J-aggregates with standard ZnO-ALD results in infiltration of the metal precursor diethylzinc into the TSPP J-aggregates and induces metalation of TSPP molecules with zinc(II) ions. Formation of the metalloporphyrins was confirmed by UV/Vis absorption and mass spectrometry. Similarly, the reaction between diethylzinc and H₂TPP as substrate with a half cycle of the ALD process also resulted in zinc(II) intercalation into the porphyrin cavity. Such a half cycle is analogous to a simple vapor-phase exposure of a substrate to the precursor in a vacuum chamber. This process can therefore be considered to be vapor-phase metalation.

[*] L. Zhang, Prof. U. Gösele, Dr. M. Knez
Max-Planck-Institut für Mikrostrukturphysik
Weinberg 2, 06120 Halle/Saale (Germany)
Fax: (+49) 345-551-1223
E-mail: lianbing@mpi-halle.de
           mknez@mpi-halle.de
Dr. A. J. Patil, Prof. S. Mann
Centre for Organized Matter Chemistry, School of Chemistry
University of Bristol (UK)
L. Li
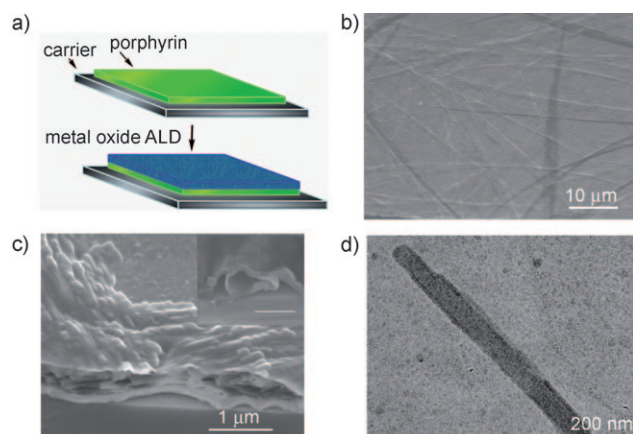Institut für Planzenphysiologie
Martin-Luther-Universität, Halle (Germany)
Dr. A. Schierhorn
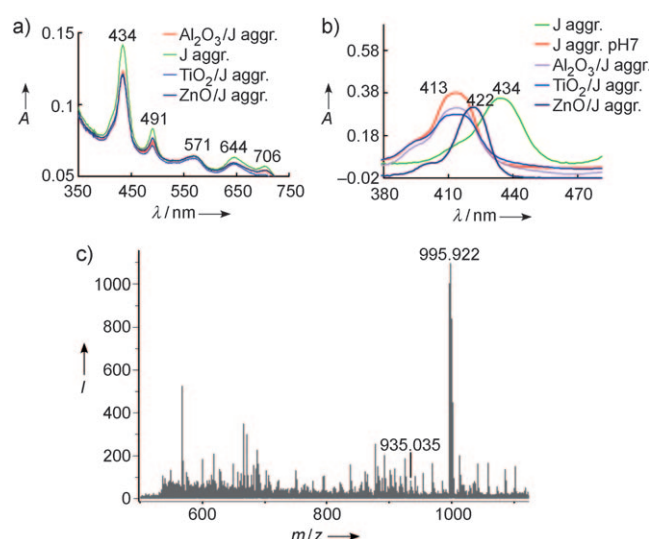Institut für Biochemie und Biotechnologie
Martin-Luther-Universität, Halle (Germany)

The use of ALD in the presence of a porphyrin-based substrate is shown in Figure 1a. SEM images of TSPP J-aggregates after ALD of TiO$_2$ (500 cycles of Ti(OiPr)$_4$/H$_2$O)

Figure 1. a) The metal oxide ALD process on porphyrins. b,c) SEM images of TSPP J-aggregates after TiO$_2$ deposition with 500 cycles of Ti(OiPr)$_4$/H$_2$O. Inset: the hollow structure of the TiO$_2$ coating after disassembly of J-aggregates following treatment with water (scale bar: 1 μm). d) TEM image of TSPP J-aggregates coated with 20 nm Al$_2$O$_3$.


Figure 2. UV/Vis absorption spectra of a) TSPP J-aggregates and J-aggregates with different metal oxides deposited by ALD and suspended in water at pH 1, and b) native and coated TSPP J-aggregates with various metal oxide ALDs suspended in water at pH7. c) MALDI-TOF mass spectrum of TSPP J-aggregates after ZnO deposition (200 cycles Et$_2$Zn/H$_2$O). ZnTSPP: m/z 995.922 ([M]$^+$), TSPP: m/z 935.035 ([M+H]$^+$).

showed a network of long bundles of coated nanofilaments on the surface of the silicon wafer (Figure 1b). Viewed in cross-section, the bundles of filament-like structures were observed below the metal oxide layer (Figure 1c). Incubating the scratched sample in water caused disassembly and dissolution of the TSPP J-aggregates at their open ends, thus producing the hollow metal oxide structures (inset, Figure 1c). TEM studies of the hybrid nanostructures after Al$_2$O$_3$ coating (Figure 1d) showed that the J-aggregate filaments were entrapped in a well-defined metal oxide shell when the coating layer remained intact during the dispersion process. Owing to its higher mass density, the metal oxide layer showed an enhanced contrast in the TEM compared to the J-aggregates. These results demonstrate that deposition of metal oxides by ALD at low temperatures takes place without significant disruption of the J-aggregate superstructure.

UV/Vis spectroscopy studies of the J-aggregate hybrid nanostructures re-suspended in water at pH 1 showed the same absorption profile as untreated J-aggregates (Figure 2a). A band at 434 nm, which is characteristic for the H$_4$TSPP^{2-} monomer, was observed, along with a red-shifted Soret band at 491 nm and broad peak at 706 nm corresponding to the J bands of the aggregates. Thus, in acidic solvent, the absorption spectra indicated that the supramolecular organization of the TSPP J-aggregate remained intact during the ALD process. Moreover, suspensions of the J-aggregate hybrid material in water at pH 7 showed absorption peaks at 413 and 515 nm, which indicate deprotonation of H$_4$TSPP^{2-} to H$_2$TSPP^{4-} and associated disassembly of the J-aggregates (Figure 2b and Supporting Information). These results indicate that the J-aggregates were still accessible to hydroxide ions, possibly because of the formation of a porous metal

oxide coating, or localized mechanical disruption in the films incurred during the re-suspension process.

Interestingly, the UV/Vis absorption spectrum of J-aggregates subjected to ZnO deposition and suspended in water at pH 7 was different to that observed after coating with Al$_2$O$_3$ or TiO$_2$. The ZnO/J-aggregate composites showed absorption maxima at 422 and 556 nm instead of the characteristic peaks for H$_4$TSPP^{2-}, H$_2$TSPP^{4-}, or J-aggregates (434 nm; 413 nm and 515 nm; 491 nm and 706 nm, respectively; Figure 2b and Supporting Information). The presence of the Soret band at 422 nm for the ZnO/J-aggregates indicates significant modification of the TSPP molecules with regard to changes to the electron density of the porphyrin ring. The results are consistent with the formation of the metalloporphyrin ZnTSPP, which has absorption maxima in aqueous solution at 422 and 556 nm.[12,13] Metalation of the porphyrin molecules by reaction of diethylzinc with TSPP during the ZnO-ALD process was confirmed by mass spectrometry (Figure 2c), in which the main signal corresponds to ZnTSPP (calculated m/z 996 [M]$^+$). The signal for the free-base TSPP (m/z 935 [M+H]$^+$) had only very low intensity, and there were no signals corresponding to TSPP conjugated with more than one zinc(II), indicating that salt formation with the sulfonato groups did not occur.

The above results were also confirmed by undertaking the ZnO-ALD process in the presence of the water-insoluble porphyrin, H$_2$TPP, which contains phenyl groups instead of the sulfonatophenyl side chains. Moreover, to further investigate the mechanism of diethylzinc infiltration and zinc(II) complexation with the porphyrin molecules, we performed a pseudo-deposition of ZnO on H$_2$TPP involving a half-cycle ALD process composed of 100 pulses of diethylzinc without water pulses. Note that such a process is identical to the

exposure of H$_2$TPP to diethylzinc vapor in a vacuum chamber, suggesting that this procedure could also be performed in suitable setups that are different from ALD. No changes were observed in the microscopic structure of the dried H$_2$TPP structures before and after the half-cycle ALD (Figure 3 a,b). After 100 pulses of diethylzinc in the ALD chamber, an absorption maximum at 420 nm in the Soret
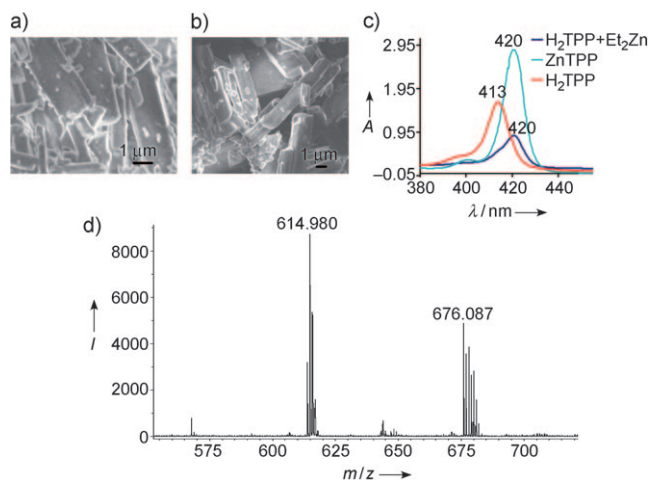
Figure 3. SEM images of H$_2$TPP dissolved in acetone and dried on a silicon wafer a) before, and b) after 100 cycles of Et$_2$Zn pulses by a half-cycle ALD. c) UV/Vis absorption spectra in acetone of H$_2$TPP, ZnTPP (99 + %, Sigma–Aldrich), and H$_2$TPP treated with Et$_2$Zn. d) MALDI-TOF mass spectrum of H$_2$TPP after treatment with a half-cycle ALD (100 pulses of Et$_2$Zn). H$_2$TPP: m/z 614.980 ([M+H]$^+$), ZnTPP: m/z 676.087 ([M]$^+$).

band region was observed, which was identical to the spectrum recorded for a standard sample of ZnTPP (Figure 3 c). Mass spectrometry analysis of H$_2$TPP after the half-cycle ALD confirmed the formation of ZnTPP (m/z 676 [M]$^+$; Figure 3 d). Identical results were also achieved when a standard ALD deposition of ZnO (with pulses of both diethylzinc and water) was applied to H$_2$TPP. TSPP could also be converted into ZnTSPP with diethylzinc pulses only (see the Supporting Information).

Our results indicate that metalation of both TSPP and H$_2$TPP can be achieved with a ZnO-ALD process, despite the different water-solubility and self-assembly properties of those different porphyrins. The conversion of the major part of TSPP molecules into their metalloporphyrin counterparts demonstrates that diethylzinc can reach the interior of compact nanostructures of the TSPP J-aggregates. The diethylzinc pulse itself was sufficient to convert the porphyrins into the corresponding metalloporphyrins, which confirms that chemical infiltration occurs during the exposure time of a half cycle, and metalation of TSPP and H$_2$TPP originates from direct decomposition of diethylzinc by the pyrrolic N-bound hydrogen atoms of the free-base porphyrins, followed by the complexation of zinc(II) (Scheme 1). Metalation was not observed after treatment with titanium and aluminum precursors. Although the reason for this is unclear, steric hindrance owing to the larger molecular size of titanium
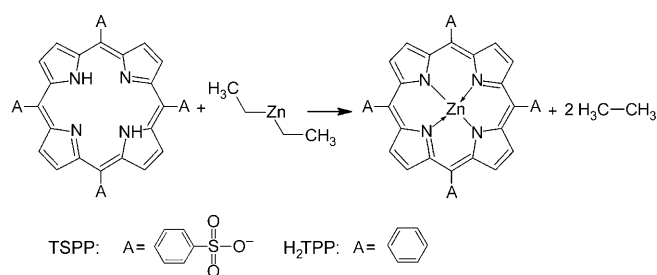
Scheme 1. Chemical reaction between diethylzinc and porphyrins TSPP and H$_2$TPP during ALD.

isopropoxide and trimethylaluminum, which exists predominantly as a dimer in the vapor phase,[14,15] may impede infiltration and successive metalation.

Metalation of porphyrin has mostly been performed in aqueous or organic media, and to overcome the slowness of the complexation reaction, either high temperature or catalysts have to be applied.[16,17] Thus, metalation of porphyrins from vapor phase could serve as a novel method to synthesize metalloporphyrins with several advantages compared to metalation in solution. In particular, the solvent-free environment of the vapor-phase reaction enables the supramolecular structures of free-base porphyrins to be metalated in situ in the absence of catalysts and at lower temperatures and short reaction times. Moreover, zinc porphyrins have higher light-to-energy efficiencies than free-base porphyrins as sensitizers for solar cells,[18–20] and several reports investigating porphyrin-dye-sensitized ZnO and TiO$_2$ solar cells have been published,[21–23] suggesting that similar configurations might be achieved in a one-step process using ALD. For example, the dye molecules could be conveniently metalated to enhance the light-electrical energy conversion efficiency, and metal oxide films of desired thickness can be deposited within an ALD chamber simply by varying the pulse sequences. In addition, infiltration of ALD precursors and induction of chemical reactions has general significance for the application of ALD in various technological fields. For example, it has been suspected that C−C double bonds were accessible to trimethylaluminum,[24] a standard ALD metal precursor, and physical infiltration in the absence of chemical interactions has been also proposed by George et al.[25,26] In another example, infiltration by ALD induced significant mechanical charges to spider silks, of which the chemical nature is not yet known in detail.[27] Certainly, the occurrence of chemical infiltration will depend on both the parameters of the ALD process and chemical properties of the template and the precursors; for example, the length of exposure and purging time, the molecule size, functional groups on the template, and the reactivity of the involved precursors and groups.

In summary, by processing standard metal oxide ALD on TSPP J-aggregates and H$_2$TPP, we have shown that the ALD precursor diethylzinc can infiltrate the bulk substrate and interact with the amine groups at the molecular level, thereby inducing metalation of the porphyrin molecules. We expect similar reactions to take place during various vapor-phase treatments using proteins, peptides, or amine-containing

polymers as substrates. For ALD applications, controlled site-specific chemical infiltration can be applied as a new method for in-situ modification of substrates, and can also provide a new aspect for precursor design. Future work will investigate the reaction kinetics, parameters affecting the infiltration depth, and the activity of standard ALD precursors to frequently used organic materials. The effect of chemical infiltration should be taken into consideration for future applications of ALD.

Experimental Section

The preparation of TSPP J-aggregates is described elsewhere.[11] For the deposition of metal oxides by ALD, a suspension of TSPP J-aggregates was dried in air on a laboratory film (Parafilm) or on a silicon wafer. The sample was subsequently transferred into the ALD chamber (Savannah 100, Cambridge Nanotechnology Inc.) and evacuated at 50°C (in the case of Parafilm) or 80°C (silicon wafer) at 0.1 Torr for 1 h to remove remaining water from the J-aggregates. After drying, the deposition of metal oxides was performed by alternating exposure to the precursors with 100, 200, or 500 cycles at 50 or 80°C at 0.2 Torr. Trimethylaluminum, titanium isopropoxide, and diethylzinc were used for the deposition of Al_2O_3, TiO_2, and ZnO as the first precursor, and water as the second precursor. The pulsing time was 0.2 s for Al_2Me_6, 1.0 s for $Ti(OiPr)_4$, 0.3 s for Et_2Zn, and 1.3 s for water. For all pulses, 60 s of exposure time and 60 s of purging time were used. Purging was carried out with argon with a flow rate of 20 standard cubic centimeters per minute. After the ALD process, the sample was examined in a scanning electron microscope (JEOL 6701F). The hybrid nanostructures were dispersed in distilled water at various pH values and studied by UV/Vis absorption spectroscopy (Lambda 25 Spectrophotometer, Perkin-Elmer Inc.; UV-1602 UV/Vis Spectrophotometer, Shimadzu) using quartz cuvettes with a 10 mm path length. For transmission electron microscopy (JEOL JEM-1010), a 10 µL aliquot of the dispersion was dropped onto carbon-coated copper grids (Plano) and allowed to stand for 2 min. The sample was air-dried after removing the excess liquid with filter paper.

The MALDI-TOF mass spectra were acquired with an Ultraflex II TOF-TOF mass spectrometer (Bruker Daltonics). For the sample preparation, 0.5 µL of a saturated solution of α-cyano-4-hydroxycinnamic acid in acetone was deposited onto the sample target. A 1 µL aliquot of the sample was injected into a small drop of water previously deposited onto the matrix surface.

[1] M. Knez, A. Kadri, C. Wege, U. Gösele, H. Jeske, K. Nielsch, *Nano Lett.* **2006**, *6*, 1172.

[2] L. Niinistö, J. Päiväsaari, J. Niinistö, M. Putkonen, M. Nieminen, *Phys. Status Solidi A* **2004**, *201*, 1443.

[3] A. Sinha, D. W. Hess, C. L. Henderson, *J. Vac. Sci. Technol. B* **2006**, *24*, 2523.

[4] R. L. Puurunen, *J. Appl. Phys.* **2005**, *97*, 121301.

[5] M. Knez, K. Nielsch, L. Niinistö, *Adv. Mater.* **2007**, *19*, 3425.

[6] M. Leskelä, M. Ritala, *Angew. Chem.* **2003**, *115*, 5706; *Angew. Chem. Int. Ed.* **2003**, *42*, 5548.

[7] X-H. Liang, S. M. Geoge, A. W. Weimer, N-H. Li, J. H. Blackson, J. D. Harris, P. Li, *Chem. Mater.* **2007**, *19*, 5388.

[8] G. M. Kim, S. M. Lee, G. H. Michler, H. Roggendorf, U. Gösele, M. Knez, *Chem. Mater.* **2008**, *20*, 3085.

[9] A. Sinha, D. W. Hess, C. L. Henderson, *J. Vac. Sci. Technol. B* **2007**, *25*, 1721.

[10] R. Rotomskis, R. Augulis, V. Snitka, R. Valiokas, B. Liedberg, *J. Phys. Chem. B* **2004**, *108*, 2833.

[11] P. J. Meadows, E. Dujardin, S. R. Hall, S. Mann, *Chem. Commun.* **2005**, 3688.

[12] R. Fujiyoshi, T. Arai, M. Katayama, *J. Radioanal. Nucl. Chem.* **1994**, *185*, 133.

[13] A. Farajtabar, F. Gharib, P. Jamaat, N. Safari, *J. Chem. Eng. Data* **2008**, *53*, 350.

[14] N. Muller, D. E. Pritchard, *J. Am. Chem. Soc.* **1960**, *82*, 248.

[15] W. R. Salaneck, R. Bergman, J. E. Sundgren, A. Rockett, T. Motooka, J. E. Greene, *Surf. Sci.* **1988**, *198*, 461.

[16] R. J. Abraham, G. R. Bedford, D. McNeille, B. Wright, *Org. Magn. Reson.* **1980**, *14*, 418.

[17] M. Inamo, A. Tomita, Y. Inagaki, N. Asano, K. Suenaga, M. Tabata, S. Funahashi, *Inorg. Chim. Acta* **1997**, *256*, 77.

[18] J. Rochford, D. Chu, A. Hagfeldt, E. Galoppini, *J. Am. Chem. Soc.* **2007**, *129*, 4655.

[19] M. Tanaka, S. Hayashi, S. Eu. , T. Umeyama, Y. Matano, H. Imahori, *Chem. Commun.* **2007**, 2069.

[20] J. Jasieniak, M. Johnston, E. R. Waclawik, *J. Phys. Chem. B* **2004**, *108*, 12962.

[21] J. Rochford, E. Galoppini, *Langmuir* **2008**, *24*, 5366.

[22] Q. Zhao, M. Yu, T. Xie, L. Peng, P. Wang, D. Wang, *Nanotechnology* **2008**, *19*, 245706.

[23] A. Forneli, M. Planells, M. A. Sarmentero, E. Martinez-Ferrero, B. C. O'Regan, P. Ballester, E. Palomares, *J. Mater. Chem.* **2008**, *18*, 1652.

[24] C.-Y. Chang, F.-Y. Tsai, S.-J. Jhou, M.-J. Chen, *Org. Electron.* **2008**, *9*, 667.

[25] C. A. Wilson, P. K. Grubbs, S. M. George, *Chem. Mater.* **2005**, *17*, 5625.

[26] C. A. Wilson, J. A. McCormick, A. S. Cavanagh, D. N. Goldstein, A. W. Weimer, S. M. George, *Thin Solid Films* **2008**, *516*, 6175.

[27] S. M. Lee, E. Pippel, U. Gösele, C. Dresbach, Y. Qin, C. V. Chandran, T. Bräuniger, G. Hause, M. Knez, *Science* **2009**, *324*, 488.